

This article was downloaded by:

On: 25 January 2011

Access details: *Access Details: Free Access*

Publisher *Taylor & Francis*

Informa Ltd Registered in England and Wales Registered Number: 1072954 Registered office: Mortimer House, 37-41 Mortimer Street, London W1T 3JH, UK



Liquid Crystals

Publication details, including instructions for authors and subscription information:

<http://www.informaworld.com/smpp/title~content=t713926090>

The phase diagram of the lyotropic nematic mesophase in the TTAB/NaBr/water system

Antonio A. de Melo Filho^a; Nader S. Amadeu^a; Fred Y. Fujiwara^a

^a Instituto de Química, Universidade Estadual de Campinas, SP CEP 13083-862, Brazil

To cite this Article Filho, Antonio A. de Melo , Amadeu, Nader S. and Fujiwara, Fred Y.(2007) 'The phase diagram of the lyotropic nematic mesophase in the TTAB/NaBr/water system', *Liquid Crystals*, 34: 6, 683 – 691

To link to this Article: DOI: 10.1080/02678290701343059

URL: <http://dx.doi.org/10.1080/02678290701343059>

PLEASE SCROLL DOWN FOR ARTICLE

Full terms and conditions of use: <http://www.informaworld.com/terms-and-conditions-of-access.pdf>

This article may be used for research, teaching and private study purposes. Any substantial or systematic reproduction, re-distribution, re-selling, loan or sub-licensing, systematic supply or distribution in any form to anyone is expressly forbidden.

The publisher does not give any warranty express or implied or make any representation that the contents will be complete or accurate or up to date. The accuracy of any instructions, formulae and drug doses should be independently verified with primary sources. The publisher shall not be liable for any loss, actions, claims, proceedings, demand or costs or damages whatsoever or howsoever caused arising directly or indirectly in connection with or arising out of the use of this material.

The phase diagram of the lyotropic nematic mesophase in the TTAB/NaBr/water system

ANTONIO A. DE MELO FILHO, NADER S. AMADEU and FRED Y. FUJIWARA*

Instituto de Química, Universidade Estadual de Campinas, Caixa Postal 6154 Campinas, SP CEP 13083-862, Brazil

(Received 7 November 2006; in final form 28 February 2007; accepted 1 March 2007)

The phase diagram of the nematic mesophase present in the tetradecyltrimethylammonium bromide/sodium bromide/water ternary system was determined. A calamitic nematic mesophase (N_C) was observed which extends to very high concentrations of electrolyte. The order parameters of the surfactant head group in the mesophases were studied by the NMR quadrupolar splitting of the deuterated surfactant. On increasing the temperature of nematic mesophases with low electrolyte concentrations, a phase separation occurs with the formation of a more highly ordered hexagonal phase and an isotropic phase. Diffusion measurements of the isotropic micellar solution by the NMR PFG method were used to estimate hydrodynamic radii at low surfactant concentrations and to study micelle diffusion as the concentration of the surfactant was increased to the liquid crystalline region. At higher surfactant concentrations, the diffusion coefficient reached a limiting value. The calamitic nematic mesophase in this surfactant/electrolyte/water system appears to be formed by long wormlike micelles.

1. Introduction

Nematic lyotropic mesophases were first observed by Lawson and Flautt [1] in the sodium decyl sulfate/sodium sulfate/decanol/water system and nematic mesophases were subsequently observed in many other systems [2]. The nematic nature of these mesophases was established by the first X-ray diffraction studies which showed that these systems are composed of micelles of discrete size with orientational order but no positional order [3–5]. Initially, two types of mesophases were observed; those with rod-like micelles forming a calamitic mesophase (N_C) and those with disc-like micelles forming a discotic mesophase (N_D). The two types of mesophase have diamagnetic and optical anisotropies with opposite signs. A distinguishing characteristic of nematic mesophases is that they spontaneously orient in magnetic fields due to their lower viscosities. These homogeneously aligned uniaxial anisotropic fluids allow one to perform many interesting NMR experiments [6].

A lyotropic biaxial nematic mesophase was first reported by Yu and Saupe in the potassium laurate/decanol/water system [7] and subsequently observed in the sodium dodecyl sulfate/decaol/water [8] and potassium dodecanoate/decylammonium chloride/water [9]

systems. Quist [10] observed two biaxial nematic mesophases with opposite diamagnetic and optical anisotropies in the sodium dodecyl sulphate/decanol/water system. Recently, a detailed study of the tetradecyltrimethylammonium bromide/decanol/water system revealed the presence of two distinct biaxial nematic mesophases [11]. On increasing the decanol content, the following sequence of phase changes was observed:

$$\text{hexagonal} - N_C - N_{bx}^+ - N_{bx}^- - N_D - \text{lamellar}.$$

The phase transitions between the two biaxial mesophases with opposite diamagnetic anisotropies are first order. However, the transition between uniaxial N_C and biaxial N_{bx}^+ nematic mesophases, both with a positive diamagnetic anisotropies, is second order as is the transition between the two mesophases with negative diamagnetic anisotropy, i.e. the discotic mesophase (N_D) and the negative biaxial mesophase (N_{bx}^-). Decanol favours a more planar aggregate interface and very small changes in the composition or temperature appear to change the shape, symmetry and orientation of the micelles.

The size and shape of micelles in nematic mesophases is still a matter of discussion. A high-resolution X-ray studies of the calamitic, discotic and biaxial nematic mesophases of the potassium laurate/decanol/water

*Corresponding author. Email: fred@iqm.unicamp.br

system concluded that the micelles in these nematic phases are all intrinsically biaxial and the occurrence of calamitic, discotic and biaxial nematic mesophases is a consequence of orientational fluctuations of these micelles [12, 13]. Neutron diffraction studies concluded that the micelles are statistically biaxial in uniaxial nematic mesophase and, furthermore, that decanol is not homogeneously distributed in the micelles [14].

Quist *et al.* [15] studied the sodium dodecyl sulfate/decanol/water systems and obtained values around 3–4 for the axial ratio $\rho = b/a$, a being the shorter and b the longer axis for a micelle in nematic phase. These results were based on a model used to calculate the effect of diffusion of quadrupolar spins on the surface of the micelle on NMR relaxation times [16]. Other studies [17] of the calamitic nematic mesophase in this system concluded that the micelles are biaxial with axial ratios of $\rho \approx 3$ –5. Similar studies of the discotic mesophase in the decyl sulfate/decanol/water system found axial ratios of 4–6 in the nematic region, which surprisingly increased to 8 in the isotropic phase [18]. Recently, an analysis of the NMR T_2 dispersion profiles of $^{23}\text{Na}^+$ in both calamitic and discotic nematic mesophases of the sodium dodecyl sulfate/decanol/water system indicated that intrinsically biaxial micelles are present in these uniaxial phases [19].

Several ternary surfactant/electrolyte/water systems have been shown to form N_C nematic mesophases [20]. However, no detailed phase diagrams have been reported for surfactant/electrolyte/water ternary systems except for the decylammonium chloride/ammonium chloride/water system [21]. However, this system seems to be an exception since this system forms a N_D nematic mesophase. This behaviour is probably due to the small ionic head group volume of this surfactant, which favours the formation of planar micellar surfaces. No information regarding the size and shape anisotropy of the micelles in the calamitic nematic mesophases present in surfactant/electrolyte/water system seems to be available. Studies of dilute micellar solutions have shown that the micelles present above the cmc become cylindrical in shape and can form long wormlike flexible micelles in the presence of an electrolyte [22, 23].

In the present study, the phase diagram of the tetradecyltrimethylammonium bromide/sodium bromide/water system was determined. The phase diagram presents a rather extensive calamitic nematic region, which extends to very high electrolyte concentrations. The order parameter of the polar head of the surfactant was determined in order to study changes in the partial orientation of the micelles in the mesophases with concentration and temperature. Diffusion coefficients of the micelles in isotropic micelle solutions were

measured by the NMR pulse field gradient technique in order to study the growth of the micelles in isotropic solutions up to the formation of mesophases.

2. Experimental

Tetradecyltrimethylammonium bromide (TTAB) (Aldrich, 99%) was recrystallized twice in mixtures of ethyl acetate (Merck, PA) and ethanol (Merck, PA), and dried under vacuum. *n*-Decanol (Eastman Kodak) was distilled under vacuum with a Vigreux column and middle fraction was collected. Sodium bromide (Ecibra, PA) was dried at 100°C.

TTAB- d_3 was prepared by mixing equimolar quantities of tetradecylamine (Aldrich, 96%) and iodomethane- d_3 (Aldrich, 99.5+ at. % D) with potassium bicarbonate (Carlo Erba, P.A.) in methanol (Merck, P.A.) at 5°C. After 24 h of reaction, an excess of CH_3I (Aldrich, P.A.) was added to achieve exhaustive methylation. The tetradecyltrimethylammonium iodide obtained was reacted with silver oxide in methanol, filtered and the hydroxide neutralized with hydrobromic acid. After drying, the TTAB- d_3 was recrystallized from ethyl acetate with yield of 82%.

The samples were prepared by mixing the components in a small test tube and stirring. Centrifugation was used to remove foam. The water used contained 10% deuterium oxide unless otherwise indicated.

The ^2H and ^{23}Na NMR spectra were observed on a Varian Gemini 2000 spectrometer with a magnetic field of 7.06 T and frequencies of 300 MHz for ^1H , 46 MHz for ^2H and 79.4 MHz for ^{23}Na . The sign of the diamagnetic anisotropy ($\Delta\chi = \chi_{\parallel} - \chi_{\perp}$) was determined by comparing the initial powder pattern of the non-oriented mesophase with the spectrum of the homogeneously aligned sample. These nematic mesophases normally require several minutes to become well oriented. Very viscous mesophases were heated and cooled in the magnet to obtain a homogeneous alignment. Nematic mesophases with a positive diamagnetic anisotropy align with the optic axis (director) parallel to the field, whereas mesophases with a negative anisotropy align with the director perpendicular to the field. The errors in the determination of the quadrupolar splittings were less than 1%. Hexagonal mesophases do not present any appreciable orientation except in the biphasic hexagon-nematic region.

The texture of the mesophases was analysed in an Olympus optical microscope model CBA-K using polarized light. The samples were placed between two lamellar plates with thickness of 0.2 mm or in sample holders with circular concave cavities with 16 mm diameters and a maximum depth of 0.5 mm. An

Olympus PM-6 camera with Kodak 100ASA 35 mm colour films were used to obtain photographs.

For the determination of the optical anisotropy, the samples were oriented in a 1.6 T magnet with the field orthogonal to the slide surface for 12 h prior to the analysis. The optical anisotropy was determined by conoscopic observations with a Zeiss model Axiophot petrographic microscope using a gypsum lambda plate.

The translational diffusion of the surfactant was measured in the isotropic domain using the pulsed field gradient technique in NMR spectroscopy. A Varian Inova 500 NMR spectrometer was used to observe the ^1H nuclei at the frequency of 500 MHz and 25°C. The GCSTESL pulse sequence [24] was employed, varying the gradient strength among 20 values. The field gradients were calibrated using liquids with known diffusion coefficients [25]. The resulting echo intensities along with the pulse sequence parameters were used in the equation [24] that describes the echo decay and an exponential fit of the data gave us the diffusion constant. The statistical errors of the diffusion coefficients in the non-linear regression analyses were less than 1%. Binary (TTAB/water) and ternary (TTAB/NaBr/water) isotropic samples were studied with TTAB mass fractions ranging from ca. 1.5 to 35%, i.e. from diluted solutions to near the isotropic–nematic phase boundary. The samples were grouped together in seven different series, each having a constant $[\text{NaBr}]/[\text{TTAB}]$ molar ratio and variable water content. The $[\text{NaBr}]/[\text{TTAB}]$ ratio ranged from 0 (binary series) to 1.5 (highest salt concentrations used for isotropic samples).

3. Results and discussion

Phase changes were detected using the residual quadrupolar splitting observed for HOD in the ^2H NMR spectrum. The quadrupolar splitting of the Na^+ ion in the ^{23}Na spectrum was also used to confirm the phase changes in the ternary systems. Figure 1 shows the results for the binary TTAB/water system prepared using water with 10 wt % D_2O . The hexagonal–nematic and nematic–isotropic phase changes are clearly first order. The hexagonal mesophase extends down to about 25% water where a solid TTAB phase is present. This is consistent with the phase diagram previously published for this binary system which also found that a lamellar phase at lower water content is only formed at temperatures above 50°C [26]. The nematic mesophase is present in an extremely narrow concentration range in the binary system (from 61.2 to 61.8% of water containing 10% D_2O). The formation of a nematic mesophase in this binary system has been previously reported, [27, 28] as well as in the similar

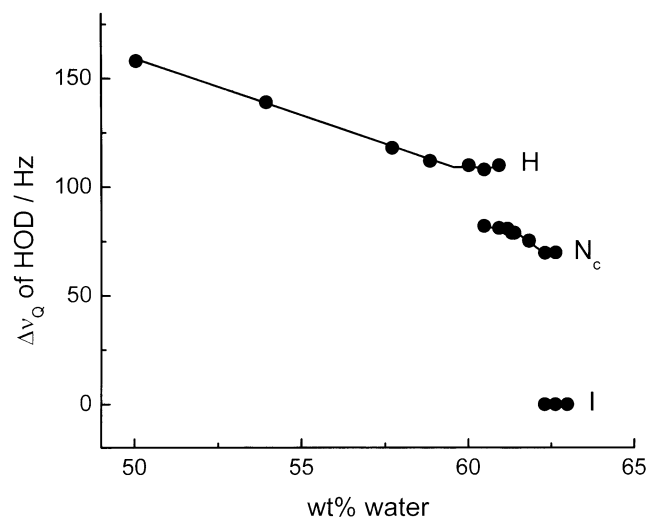


Figure 1. Determination of the phase boundaries of the TTAB/water binary system at 22°C using the residual ^2H quadrupolar splittings of DOH. The hexagonal mesophase does not spontaneously orient in the magnetic field except in the nematic–hexagonal biphasic region. All quadrupolar splittings are for a 0° orientation of the director with the magnetic field. The water used to prepare the solutions contained 10% D_2O . (Symbols: H, hexagonal; N_C : calamitic nematic; I, isotropic).

hexadecyldimethylethylammonium bromide/water binary mixture [29].

With the addition of NaBr, the ternary system forms a rather extensive nematic region. Figure 2 presents the phase diagram as a function of composition in mass fraction for the TTAB/NaBr/water system. The nematic

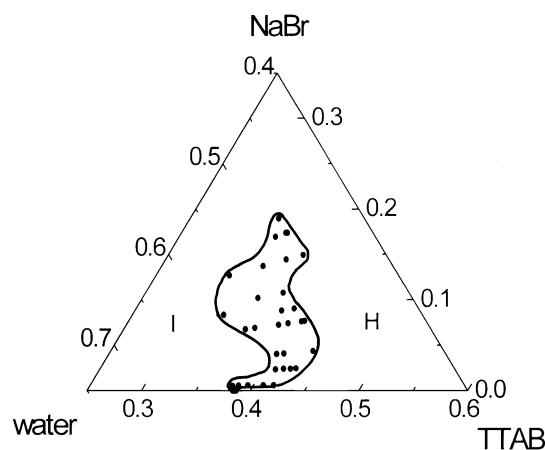


Figure 2. The ternary phase diagram of the TTAB/NaBr/water system at 22°C. Coordinates are in mass fraction and the water used to prepare the samples contained 10% D_2O . The points represent some representative homogeneous nematic mesophases (N_C) observed. The hexagonal–nematic and nematic–isotropic biphasic regions, which extend over approximately 1% water content, are not shown.

mesophases homogeneously orient in magnetic fields with the director parallel to the magnetic field and thus have a positive diamagnetic anisotropy. Conoscopic studies showed that this mesophase has a negative optical anisotropy. The N_C nematic region is boarded by an isotropic micellar solution on the water rich side and by a hexagonal mesophase on the water poor side. Narrow biphasic regions were observed for the first order phase transitions between the nematic-hexagonal and the nematic-isotropic phases. Figure 1 shows that the biphasic regions extend over approximately 1% water content for the binary system. Biphasic regions with similar extensions were observed for the ternary system containing NaBr.

As shown in figure 2, the addition of NaBr results in an extensive nematic region. Surprisingly, the nematic phase is formed up to 19% of electrolyte. This concentration represents about 3.8 mol of NaBr per kilogram of water and a surfactant:electrolyte molar ratio of 1:1.6. This nematic mesophase does not seem to be very sensitive to the nature of the electrolyte. Nematic mesophases were also prepared using 4% NaCl, 4% NaOH and 2% HCl as the electrolyte.

The order parameter in these uniaxial anisotropic fluids was studied using the quadrupolar splitting of the CD_3 group of TTAB- d_3 . The order parameter of the water is often difficult to interpret since the binding sites on the micelle surface can change in an unpredictable manner. For example, in the TTAB/decanol/water system, the order parameter of D_2O was observed to decrease in magnitude with increasing temperature, become zero and then increase in magnitude due to changes in sign of the order parameter. [30]. The deuterium quadrupolar splitting ($\Delta\nu_Q$) for the C–D bond in the $N(CD_3)_3$ moiety in an oriented anisotropic sample is related to the order parameter by the relation,

$$\Delta\nu_Q = 3/2(e^2qQ/h)S_{CD}^{1/2}(3 \cos \Omega - 1) \quad (1)$$

where e^2qQ/h is the quadrupole coupling constant and Ω is the angle between the director and the applied magnetic field. The expression is valid for an axially symmetric electric field gradient which is a good approximation for the C–D bond. The order parameter of the carbon–deuterium bond is given by [31]:

$$S_{CD} = 1/2 \langle 3 \cos^2 \theta - 1 \rangle \quad (2)$$

where θ is the angle between C–D axis and the mesophase director and the angular brackets indicate an average value over the molecular motion. Due to the cylindrical symmetry, the order parameter of the C_x –N

bond can be expressed as,

$$S_{CN} = 1/2(3 \cos^2 \theta_1 - 1) 1/2(3 \cos^2 \theta_2 - 1) S_{CD} \quad (3)$$

where θ_1 and θ_2 are the C–C–D and C–C–N bond angles in the $-CH_2N(CD_3)_3$ moiety, which are approximately equal to the tetrahedral angle.

The observed order parameter is an average for the instantaneous orientations that the bond axis experiences since the lifetime of these conformations is much shorter than the NMR observation timescale. The rapid molecular motions of the surfactant head group reduce the order parameter. These motions can be divided into the movement of the moiety inside the micelle, the diffusion on the surface of the micelle and the oscillations of the micelle about its average orientation. If one assumes that the packing and molecular motion of the surfactant incorporated in the micelle changes little, the order parameter with respect to an axis normal to the micellar interface should be the same in all systems. Therefore, the variation in the order parameter of the head group should reflect the partial orientation of the micelle with respect to the director, which depends on the size, shape and flexibility of the micelles.

In a previous study of the TTAB/decanol/water system [11] the addition of the alcohol to the binary mixture was shown to form a large region in the phase diagram where a nematic calamitic mesophase is present. Further addition of decanol induces a transition to a nematic discotic mesophase (N_D) after passing through two small regions of two different biaxial mesophases intermediating the uniaxial phases. This is an indication that decanol induces a lowering of the aggregates surface curvature and changes the shape and symmetry of the micelles. In the ternary mixture containing an electrolyte, only one type of nematic phase is formed. Electrolytes do not seem to change the micellar shape so strongly. The most evident effect of electrolytes seems to be extending the nematic region with respect to the water content and temperature range. Electrolytes stabilize the nematic phase presumably due to the screening of the electrostatic repulsion between micelles. A reduced repulsion would favour the formation of a nematic mesophase rather than a hexagonal packing of the micelles. The effect of the electrolyte concentration is shown in figure 3. An increase in electrolyte concentration in samples with a constant TTAB:water ratio does not have a very strong effect on the order parameter of the micelles, which indicates that the electrolyte does not provoke a dramatic change in the micelle size.

The temperature dependence of these calamitic mesophases varies with the electrolyte concentration. Above 4% NaBr, the temperature seems to have a small

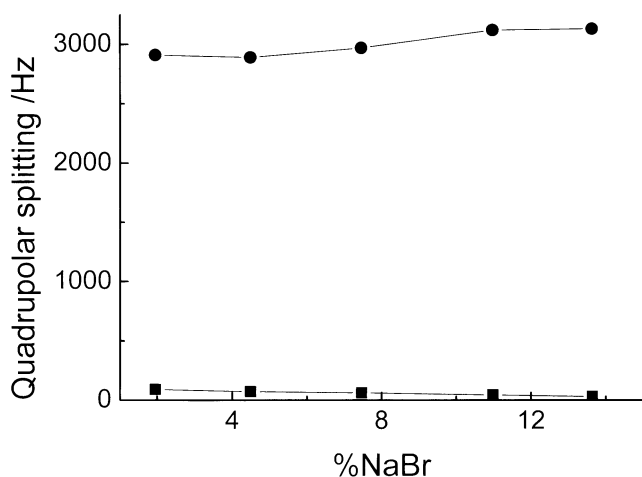


Figure 3. The ^2H quadrupolar splitting of the CD_3 group of TTAB- d_3 as a function of NaBr concentrations in a nematic calamitic mesophase with a constant ratio of $[\text{TTAB}]/[\text{H}_2\text{O}]=0.037$ at 22°C . The water contained 0.2% D_2O and approximately 4% of the TTAB was labelled. The rather small change in the parameter order of the C–D bond in the range of concentrations studied indicates that the micelle order parameter is not very sensitive to the electrolyte concentration.

effect on the order parameter. Figure 4 presents the effect of the temperature on the TTAB/NaBr/water nematic mesophase using the quadrupolar splitting of the CD_3 group of TTAB- d_3 . The N_C mesophase with this water content extends from about 5 to 60°C . Between 60 and 75°C , a biphasic nematic–isotropic system is present and above 75°C the system becomes

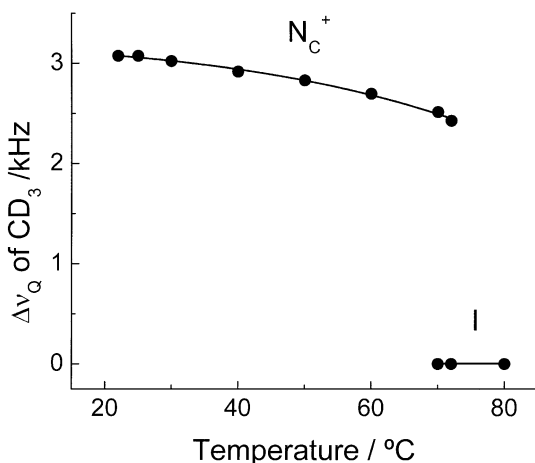


Figure 4. The ^2H quadrupolar splitting of the CD_3 group in TTAB- d_3 as a function of temperature in a sample containing 53.00 wt % water, 4.11% of NaBr and $[\text{TTAB}]/[\text{H}_2\text{O}]=0.042$. Approximately 3% of the TTAB was TTAB- d_3 and the water contained 0.1% D_2O . The modest temperature dependence of the order parameter of the C–D bond is characteristic of this nematic mesophase and was observed in all samples with more than 3% NaBr.

completely isotropic. A very similar behaviour was observed for NaBr concentrations from 4 to 19% in samples with the same surfactant/water ratio as the sample in figure 4. There is a rather small decrease of the order parameter of the head group over the nematic range, which is a characteristic of this calamitic mesophase. The hexagonal mesophase has even smaller temperature dependence. Apparently, temperature does not have a strong effect on the size and mobility of the micelles in both phases.

However, mesophases with electrolyte concentrations lower than 4% presented a more complex behaviour. In this concentration range, the nematic phase forms an isotropic–nematic biphasic system followed by an isotropic–hexagonal region at higher temperatures. Figure 5 shows the temperature dependence of a nematic mesophase with 0.83% NaBr.

The phase diagram at very low electrolyte concentrations is complex and is sensitive to the electrolyte and water concentrations. Figure 6 shows the temperature dependence of a nematic mesophase with 0.62% NaBr and less water than the sample in figure 5. In this case, a biphasic region with the nematic and hexagonal mesophases in equilibrium is formed on increasing the temperature followed by a surfactant-rich hexagonal phase in equilibrium with an isotropic phase. This behaviour has been previously observed in other ternary systems containing an electrolyte [20]. Also the presence of the nematic, hexagonal and isotropic phases in equilibrium was observed in some samples with low

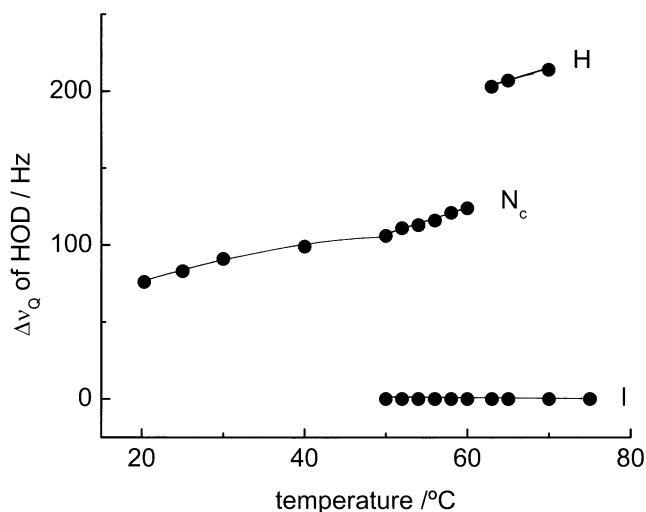


Figure 5. The ^2H quadrupolar splitting HOD as a function of temperature in a sample containing 56.48 wt % water, 2.35% of NaBr and $[\text{TTAB}]/[\text{H}_2\text{O}]=0.039$. The water contained 10% D_2O . Nematic mesophases with less than 3% electrolyte present a nematic–isotropic biphasic region followed by a hexagonal–isotropic region on increasing the temperature.

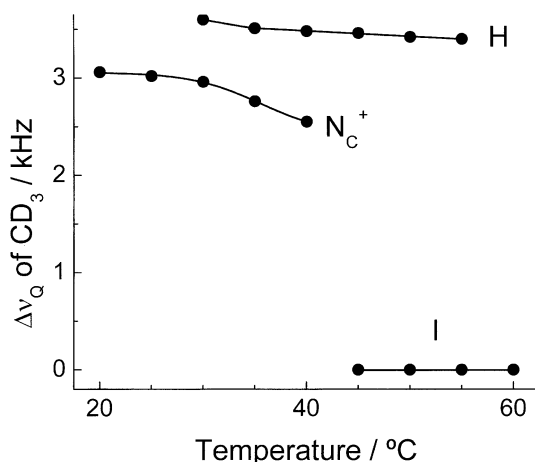


Figure 6. The ^2H quadrupolar splitting of the CD_3 group of TTAB- d_3 as a function of temperature in a sample containing 56.25% water, 0.61% of NaBr and $[\text{TTAB}]/[\text{H}_2\text{O}]=0.041$. The water contained 0.2% D_2O . This nematic mesophase presents a nematic–hexagonal biphasic region followed by a hexagonal–isotropic region on increasing the temperature.

electrolyte concentrations. Figure 7 presents a simplified phase diagram of the temperature where the fine detail in the low electrolyte region are omitted.

Statistical mechanical calculations based on cylindrical micelles [32–34] have predicted a behaviour analogous to the one observed here. Below a critical temperature, the formation of the isotropic, nematic and hexagonal phases depends on the volume fraction

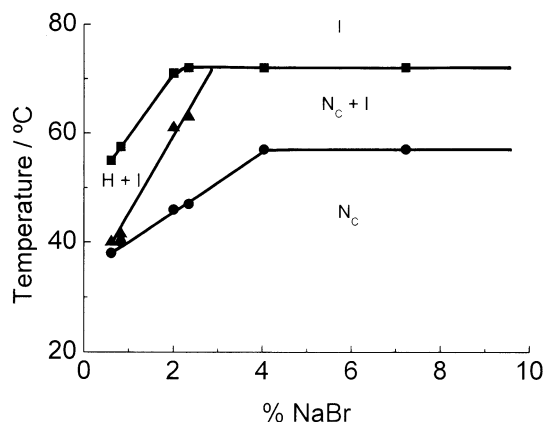


Figure 7. Phase diagram of the TTAB/NaBr/water system as a function of temperature determined using the residual quadrupolar splittings of HOD, TTAB- d_3 or the Na^+ ion. The data in this phase diagram are for a constant molar ratio of $[\text{TTAB}]/[\text{H}_2\text{O}] \approx 0.039$ and the diagram can be extrapolated to 19% NaBr. The phase diagram for NaBr mass fractions of less than 1% is more complex than that shown in the figure. In samples with less water, nematic and hexagonal mesophases in equilibrium were observed followed by a nematic–hexagonal–isotropic region and then a hexagonal–isotropic region as the temperature was increased.

(v_p) of the surfactant and above the critical temperature, the nematic mesophase is not formed. At higher temperatures where the micelle lengths are shorter, the nematic phase is not stable. The phase diagram published by Taylor and Herzfeld [33] for rod-like micelles with a polydispersed aggregate size distribution predicts that a nematic–isotropic transition occurs on increasing the temperature at low v_p values. At intermediate v_p values, a transition of the nematic phase into an extensive isotropic–hexagonal biphasic region occurs on increasing temperature. At higher values of v_p , there is a nematic–hexagonal phase transition through a biphasic region. This biphasic region is narrow at low temperatures and broad at high temperatures.

Although the theoretical calculations do not treat ionic surfactants, the behaviour predicted by the calculations is analogous to the behaviour observed in this study when the temperature and the electrolyte concentration are changed. High concentrations of electrolyte reduce the electrostatic inter-micellar interaction which should have the same effect as reducing the effective volume fraction. For this reason, at high electrolyte concentrations, only a nematic–isotropic phase transition is observed on increasing the temperature. This is the behaviour predicted for low effective volume fractions.

Lowering the electrolyte concentration corresponds to increasing the electrostatic repulsion, which has the same effect as increasing in effective volume fraction. For larger volume fractions, the calculations predict that increasing the temperature will result in a phase separation forming a surfactant-rich hexagonal mesophase in equilibrium with an isotropic phase. This behaviour was observed in several samples containing less than 3% NaBr. The transformation of a nematic mesophase into a nematic/hexagonal biphasic system followed by hexagonal/isotropic region as the temperature is increased is shown in figures 6 and 7. This behaviour is also predicted by the theoretical calculations [33].

The growth of the micelles present in the isotropic phase was studied by diffusion measurements. The diffusion coefficients (D) of the TTAB molecules were measured by the PFG-NMR technique. The surfactant concentration ranges from the diluted region (ca. 1.5% TTAB mass fraction) to near the isotropic–nematic phase transition (ca. 35% TTAB mass fraction). Results for two ternary sample series with a constant salt/surfactant molar ratio are shown in figure 8. Seven sample series were studied with $[\text{NaBr}]/[\text{TTAB}]$ ratios ranging from 0 to 1.5.

Figure 8 reveals two regimes: a diluted one, where the surfactant diffusion decreases sharply as the surfactant

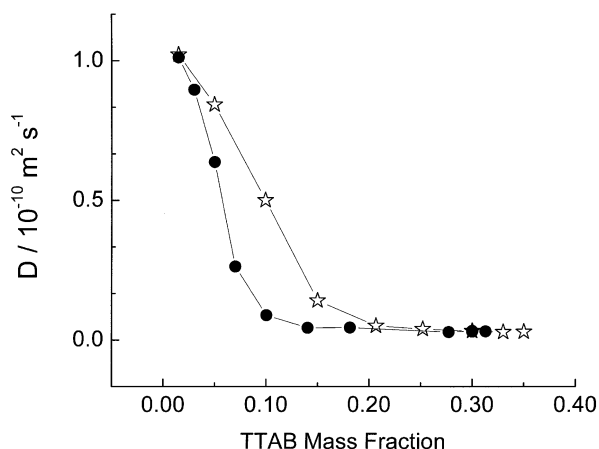


Figure 8. The diffusion coefficients of TTAB in isotropic micellar solutions of TTAB/NaBr/water systems measured by the PFG NMR technique. The stars are for samples with $[\text{NaBr}]/[\text{TTAB}]=0.33$, and the circles are for samples with $[\text{NaBr}]/[\text{TTAB}]=1.14$. Two distinct regimes are observed, a diluted one, with a strong dependence of the diffusion on concentration and a concentrated one, with a constant diffusion coefficient.

concentration increases, and a concentrated one, where the diffusion is approximately independent of the mass fraction. This two-regime behaviour was seen in all the other sample series studied. The transition from the diluted to the concentrated regime occurs at ca. 20% TTAB for the binary TTAB/water series and at ca. 10% TTAB for the ternary TTAB/NaBr/water system having $[\text{NaBr}]/[\text{TTAB}]=1.5$, the highest ratio studied. The series with intermediate salt concentration undergo the transition of regimes at intermediate TTAB mass fractions (10–20%). The higher the salt/surfactant molar ratio, the lower the TTAB mass fraction at which the system reaches the concentrated regime. The two-regime behaviour has also been observed for other systems [35–37].

To interpret the diluted regime, one can assume that the surfactant free monomer diffusion is not important. The surfactant critical micelle concentration (cmc) is 0.13% TTAB mass fraction and the monomer diffusion coefficient was measured to be $D=1.5 \times 10^{-10} \text{ m}^2 \text{ s}^{-1}$, not far from the values of our 1.5% TTAB solutions figure 7. The surfactant lateral diffusion along the micelle is not important for small micelles so we can equate the diffusion of the micelles with the surfactant molecules. Thus, we can use the Stokes–Einstein equation:

$$D_{obs} = D_{mic} = kT/6\pi\eta R_h \quad (4)$$

where D_{obs} is the observed diffusion coefficient, D_{mic} is the micelle diffusion, k is the Boltzman constant, T is the temperature, η is the viscosity of a submicellar

solution close to the cmc and R_h is the hydrodynamic radius. This equation applies as long as the obstruction effect caused by the colloidal particles is not strong. To ensure that we are working under this condition, we will focus on the more dilute region of the isotropic domain from 5 to 10 wt % of TTAB, which is still far from the concentration where the entanglement of the micelles is apparent. The hydrodynamic radii for two series by applying these approximations are shown in figure 9. Similar hydrodynamic radii were found by Weican *et al.* [38] for micelles in the CTAB/KBr/water system.

In the concentration range in figure 9 is well above the TTAB second cmc, which was measured [23] to be 0.77% (0.023 mol l^{-1}) for the TTAB/water system at 25°C. This value is much lower when salt is added. Therefore, we will use the spherocylinder model [39] to interpret the diffusion of the micelles. Yamakawa and Fujii [40] used hydrodynamics concepts to calculate the friction coefficient (f) of a wormlike chain with a defined diameter. They found

$$f = \frac{9\pi\eta}{4} \left(\frac{\pi}{6}\right)^{1/2} L^{1/2} \quad (5)$$

where L is the micelle length. If we apply this expression in the Einstein equation for diffusion ($D=kT/f$), we have

$$D_{mic} \propto L^{-1/2}. \quad (6)$$

This relationship can be used to calculate the elongation of the wormlike micelles in the diluted regime. Our data show that the micelles are six times

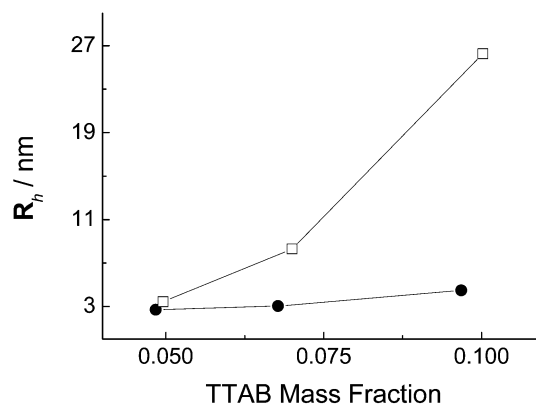


Figure 9. The hydrodynamic radii of micelles in the isotropic diluted regime of the TTAB/NaBr/water system. The circles (●) indicate samples with $[\text{NaBr}]/[\text{TTAB}]=0.05$ and the squares (□) indicate samples with $[\text{NaBr}]/[\text{TTAB}]=1.14$. A faster micelle elongation with the addition of surfactant was observed at higher NaBr/TTBA ratios for all six series studied (only two sample series are shown in the figure).

longer at 15% than at 5% TTAB for the series with $[\text{NaBr}]/[\text{TTAB}] = 0.05$. When this molar ratio is 0.33, the micelles are ca. 40 times longer at 15% as compared to 5% and for $[\text{NaBr}]/[\text{TTAB}] = 1.14$, the micelles are about 60 times longer at 10% compared to their length at 5%. These estimates are obviously subject to some error because we did not include the obstruction effect in our treatment. However, this effect should be small at this concentration range and our figures should be a reasonable approximation and the data give a good idea of how an increase in the salt/surfactant molar ratio facilitates the micelle elongation as the surfactant concentration increases.

In the concentrated isotropic regime, the micelles are already long and entangled. This situation has been previously reported for this and similar systems [26, 36]. Colloidal diffusion is very restricted by the dense population of wormlike micelles in this case. Thus, other phenomena become important such as the lateral diffusion of the surfactant along the micelle, micelle reptation and micelle scission and recombination [41, 42]. The lateral diffusion determines the surfactant displacement and it is reasonably concentration independent, which is consistent with the presence of a plateau in our diffusion curves in figure 8. The magnitude of the diffusion coefficient in the plateau region is similar to that observed for dodecyltrimethylammonium chloride in a bicontinuous cubic phase [43].

The results obtained in this study indicate that the nematic calamitic mesophase formed in the TTAB/electrolyte/water system is composed of long cylindrical micelles. This appears to be characteristic of ternary surfactant/electrolyte/water systems. The limited data for ternary systems containing potassium dodecanoate or decyl sulfate salts are very similar to the system studied here [20]. The characteristics of these nematic mesophases are distinctively different than those of the nematic mesophases form by the addition of a long-chained alcohol. The studies cited in the introduction have indicated the presence of finite micelles with low shape anisotropies and with symmetries which are very sensitive to the composition of the mesophases.

Acknowledgements

The authors thank FAPESP for financial support and AAM and NSA wish to thank CAPES and FAPESP, respectively, for fellowships.

References

- [1] K.D. Lawson, T.J. Flautt. *J. Am. chem. Soc.*, **89**, 5489 (1976).
- [2] B.J. Forrest, L.W. Reeves. *Chem. Rev.*, **81**, 1 (1981).
- [3] L.Q. Amaral, C.F. Pimentel, M.R. Tavares, J.A. Vanin. *J. chem. Phys.*, **71**, 2940 (1979).
- [4] J. Charvolin, A. Levelut, E.T. Samulski. *J. Phys. Lett.*, **40**, L587 (1979).
- [5] A.M. Figueiredo Neto, L.Q. Amaral. *Mol. Cryst. liq. Cryst.*, **74**, 109 (1981).
- [6] C.L. Ketrapal, A.C. Kunwar, A.S. Tracey, P. Dielh. In *NMR Basic Principles and Progress*, P. Dielh, E. Fluck, R. Kosfeld (Eds), Springer-Verlag, Berlin (1975).
- [7] L.J. Yu, A. Saupe. *Phys. Rev. Lett.*, **45**, 1000 (1980).
- [8] R. Bartolino, T. Chiaranza, M. Meuti, R. Compagnoni. *Phys. Rev. A*, **26**, 1116 (1982).
- [9] E.A. Oliveira, L. Liebert, A.M. Figueiredo Neto. *Liq. Cryst.*, **5**, 1669 (1987).
- [10] P.O. Quist. *Liq. Cryst.*, **18**, 623 (1995).
- [11] A.M. Melo Filho, A. Laverde Jr., F.Y. Fujiwara. *Langmuir*, **19**, 1127 (2003).
- [12] A.M. Galerne, A.M. Figueiredo Neto, J. Liébert. *J. chem. Phys.*, **87**, 1851 (1987).
- [13] Y. Galerne. *Mol. Cryst. liq. Cryst.*, **165**, 131 (1988).
- [14] Y. Hendrix, J. Charvolin, M. Rawiso. *Phys. Rev. B*, **33**, 3534 (1986).
- [15] P.-O. Quist, B. Halle, I. Furó. *J. chem. Phys.*, **96**, 3875 (1992).
- [16] B. Halle. *J. chem. Phys.*, **94**, 15 (1991).
- [17] P.-O. Quist. *J. Phys. chem.*, **100**, 4976 (1996).
- [18] I. Furó, B. Hale. *Phys. Rev. E*, **51**, 466 (1995).
- [19] C.R. Rodrigues, D.J. Pusiol, A.M. Figueirdo Neto, C.A. Martin. *Phys. Rev E*, **69**, 041708 (2004).
- [20] F.Y. Fujiwara, L.W. Reeves. *J. phys. Chem.*, **84**, 653 (1980).
- [21] M.R. Rizzatti, J.D. Gault. *J. Colloid Interface Sci.*, **110**, 258 (1986).
- [22] M.E. Cates, S.J. Candau. *J. Phys. condensed Matter*, **2**, 6869 (1990).
- [23] T. Imae, S. Ikeda. *J. phys. Chem.*, **90**, 5216 (1985).
- [24] C.S. Johnson Jr. *Prog. NMR Spectrosc.*, **34**, 203 (1999).
- [25] M. Holtz, H. Weingärtner. *J. Magn. Resonance*, **92**, 115 (1991).
- [26] T. Wärnheim, A. Jönsson. *J. Colloid Interface Sci.*, **125**, 627 (1988).
- [27] N. Boden, K. Radley, M.C. Holmes. *Mol. Phys.*, **42**, 493 (1981).
- [28] P. Photinos, S.Y. Xu, A. Saupe. *Phys. Rev. A*, **42**, 865 (1990).
- [29] H.D. Dorfler, C. Gorgens. *Tenside Surfactant Detergents*, **37**, 17 (2000).
- [30] G. Arabia, G. Chidichimo, A. Golemme, P. Ukleja. *Liq. Cryst.*, **10**, 311 (1991).
- [31] A. Saupe. *Z. Naturforsch.*, **19a**, 161 (1964).
- [32] R. Hentschke, J. Herzfeld. *Phys. Rev. A*, **94**, 1148 (1991).
- [33] M.P. Taylor, J. Herzfeld. *Phys. Rev. A*, **43**, 1892 (1991).
- [34] P. van der Schoot. *J. chem. Phys.*, **104**, 1130 (1996).
- [35] J. Narayanan, W. Urbach, D. Langevin, C. Manohan, R. Zana. *Phys. Rev. Lett.*, **81**, 228 (1998).
- [36] N. Morié, W. Urbach, D. Langevin. *Phys. Rev. E*, **51**, 2150 (1995).

- [37] T. Kato, T. Terao, T. Seimiya. *Langmuir*, **10**, 4468 (1994).
- [38] Z. Weican, L. Ganzuo, M. Jianhai, S. Qiang, Z. Liqiang, L. Haojun. *Chin. Sci. Bull.*, **45**, 1854 (2000).
- [39] G. Porte, Y. Poggi, J. Appell, G. Maret. *J. phys. Chem.*, **88**, 5713 (1984).
- [40] H. Yamakawa, M. Fujii. *Macromolecules*, **6**, 407 (1973).
- [41] V. Schmitt, F. Lequeux. *Langmuir*, **14**, 283 (1998).
- [42] M.E. Cates. *Europhys. Lett.*, **4**, 497 (1987).
- [43] G. Lindblom, G. Oradd. *Prog. NMR Spectrosc.*, **26**, 483 (1994).